Available online at www.sciencedirect.com
ScienceDirect
Trans. Nonferrous Met. Soc. China 25(2015) 397−404
Transactions of Nonferrous Metals Society of China
www.tnmsc.cn

Influence of high frequency vibration on microstructure and mechanical properties of TIG welding joints of AZ31 magnesium alloy

Tong WEN, Shi-yao LIU, Shi CHEN, Lan-tao LIU, Chen YANG

College of Materials Science and Engineering, Chongqing University, Chongqing 400044, China

Received 10 February 2014; accepted 28 May 2014

Abstract: A device for superimposing vibration on workpiece in both horizontal and vertical directions during tungsten-arc inert gas (TIG) welding was developed, with maximum power output of 2 kW at frequency of 15 kHz. AZ31 sheets with thickness of 1 and 3 mm were used in the vibratory welding. Microstructures along with the mechanical properties of the weld joints under different vibrating conditions (vibration direction, vibration amplitude and groove angle) were examined. It is observed that the grain size in welding zone decreases remarkably with the application of vibration, while the amount of second phase β-$Mg_{17}Al_{12}$ within the zone decreases slightly; meanwhile, microhardness of the weld joints, macroscopic tensile strength and elongation of the weldment increase. Vibration, especially the one along vertical direction, has more impact on the performance of the thick weldments. Influence of vibration on microstructure and mechanical properties of weldments is affected by wave energy transferring in the melt and depends on the processing and geometric parameters including amplitude and direction of vibration, thickness, and groove angles.
Key words: magnesium alloy; TIG welding; vibration; microstructure; mechanical properties

1 Introduction

Welding methods of magnesium alloys include TIG welding [1−3], MIG welding [4], friction welding [5], laser welding or laser-TIG hybrid welding [6,7], electron beam welding [8], resistance welding [9], and so on. Among these technologies, TIG welding is the most widely used one due to large penetration and small consumption of electrodes. During TIG welding of Mg alloys, clean surface of the plate can be obtained by destructing, evaporating and removing the oxide film with cathode spots. In general, however, due to the inherent properties such as strong affinity with oxygen and nitrogen, low melting point, high thermal conductivity and expansion coefficient, welding of Mg alloys is more difficult than that of the ordinary steels. Oxidation burning, porosity, crack, wide heat-affected zone (HAZ) and large welding deformation, etc., are prone to occur in the welding course, and it is difficult to obtain weld joints that can match the performances of base metal [2−4]. In the industrial environment, it is important to develop proper welding methods of Mg alloys.

For a long time, vibration, either at low or high frequency, has been utilized in the field of welding for specific purposes such as developing particular welding processes and improving quality of the welding structures. To date, numbers of researches have been carried out on the topic, for example, the utilization of vibration on welded parts to release the residual stress [10]. Vibration can also be used as energy input for the direct joining between sheets of similar or dissimilar materials [11−14]. Recently, PATEL et al [15,16] investigated the influence of ultrasonic spot welding on microstructure in a magnesium alloy.

Generally, there is insufficient energy available for activation of the microstructural changes when vibrating after the welding, whereas vibration has significant effect on the microstructure and properties of metal if it is applied during the solidification of melt [17−19]. Based on the knowledge, vibratory welding or vibratory weld conditioning (VWC), which makes the workpiece vibrate during the welding process via superimposing periodic external force on the workpiece, was developed to reduce welding residual stress and to improve the quality of weldment [20−23].

Nevertheless, as an emerging technology, vibratory

Foundation item: Project (2012ZX04010-081) supported by the National High-tech Research and Development Program of China; Project (CDJZR 12110072) supported by Fundamental Research Funds for Central Universities of China
Corresponding author: Tong WEN; Tel: +86-13018363383; E-mail: wentong@cqu.edu.cn
DOI: 10.1016/S1003-6326(15)63616-0

welding still requires further in-depth examination, from excitation equipment to factors that affect the welding process, together with the intrinsic mechanisms. In the joining of magnesium alloys, fundamental understanding on the welding with the application of vibration is lacking, and so far the effect of high frequency vibration on the fusion welding of AZ31 alloy is unknown. To this end, in the current work, a device by which high frequency vibration can be imposed on the workpiece during TIG welding was designed, and the effect of vibration on the microstructure and mechanical properties of the TIG weld joints of AZ31 sheets was investigated.

2 Experimental

Ultrasonic vibration based on piezoelectric effect is commonly used in practice since it is relatively easy to conduct and control. Furthermore, ultrasonic vibration has characteristics such as no noise emission and special functions in the fields including materials handling [24]. Figure 1 illustrates the ultrasonic-vibration apparatus designed for vibratory welding in the current work. The excitation parts include an ultrasonic generator operating at a frequency of 15 kHz with a maximum output of 2 kW, a piezoceramic vibration transducer, a tapered horn resonator and a frame. Energy (or amplitude) of the ultrasonic vibration output can be modified by adjusting position of the amplitude knob on the ultrasonic generator. When power output reaches the maximum of 2 kW, maximum amplitude along the vertical direction is about 0.003 mm at the end of tapered horn resonator [24]. The vibration transfers from the piezoceramic vibration transducer, through the tapered horn resonator and then the cushion plate, finally reaches the workpiece that is held firmly on the cushion plate with bolts.

As shown in Fig. 1, horizontal vibration (H-vib) and vertical vibration (V-vib) can be superimposed on the workpieces during the TIG welding, where the H-vib parallels to the welding line. Since rebound of the welding wire and splash of the melt were found in the preliminary test when energy output exceeded 40%A (A denotes amplitude under the maximum output), ultrasonic excitations at amplitude knob positions of 12.5%A, 25%A and 37.5%A were selected in the test.

AZ31 sheets with thickness of 1 mm and 3 mm were used in the one side TIG butt welding and the welding wire was the same alloy, which has a nominal chemical composition of Mg−2.8Al−0.9Zn−0.24Mn−0.004Fe−0.08Si (mass fraction, %). Specimens were machined to a plane size of 50 mm×40 mm, and as shown in Fig. 1(a), the weld groove angles θ are 0°, 20°, 40° and 60°, respectively. Before the operation, oxidation layers on sheet surface were wiped out with polishing and then cleaned with acetone.

Figure 2 shows the excitation device and the Panasonic YC−300WP welding machine used in the experiment. Welding speed is 20 cm/min. The alternating current is 100 A for welding AZ31 sheets with thickness of 3 mm, and is 45 A for 1 mm thickness. The specimen was fixed on a cushion plate which was connected to the excitation device. There was no preheating before welding.

3 Results and discussion

3.1 Structures of welding joints

Figure 3 shows the macroscopic topography of the TIG welding joints of AZ31 sheets. It can be found that the sheets are penetrated, whether there is vibration or not in the welding. Figure 4 gives the microstructures of the base metal and the welded zone of AZ31 sheets with 3 mm thickness under vibration amplitude of 25%A. Figure 5 shows the microstructures of the welded zone of sheets with 1 mm thickness under different vibration amplitudes.

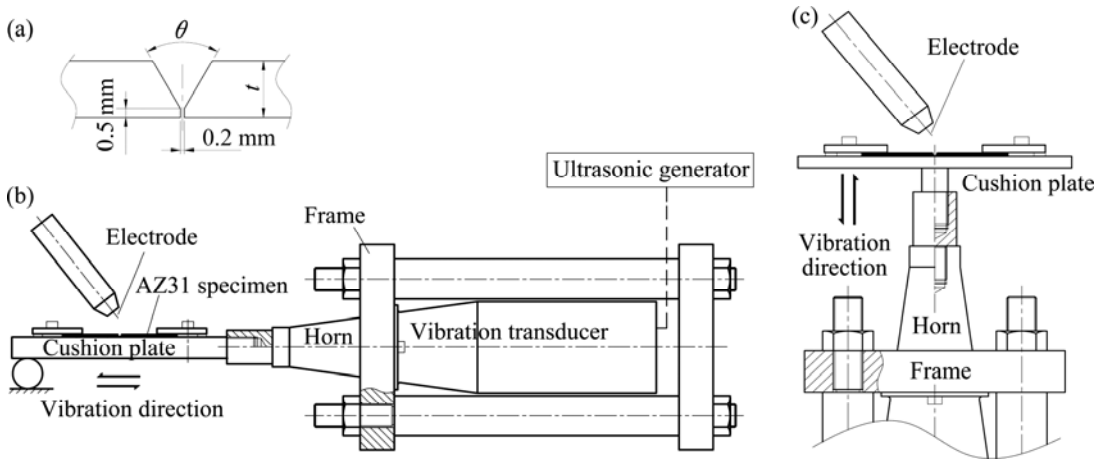

Fig. 1 Schematic diagrams of set-up for welding with high-intensity ultrasonic emission: (a) Shape and dimension of welding groove; (b) For H-vib; (c) For V-vib

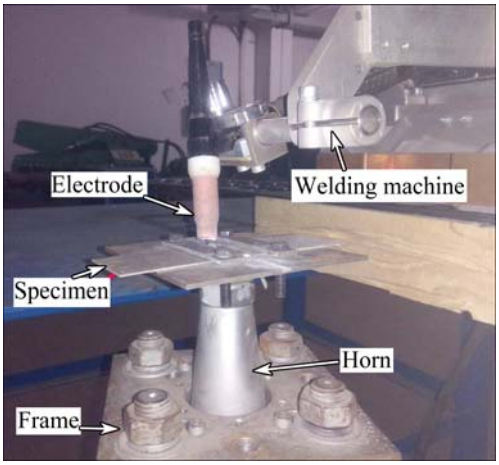

Fig. 2 Device for vibratory TIG welding

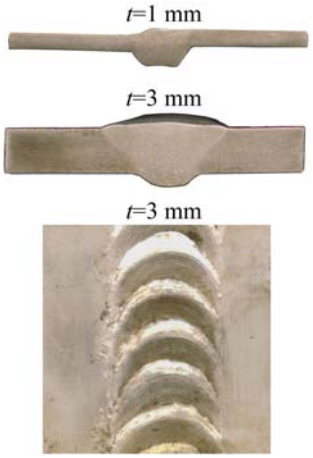

Fig. 3 Macro-morphology of vibratory welded seam

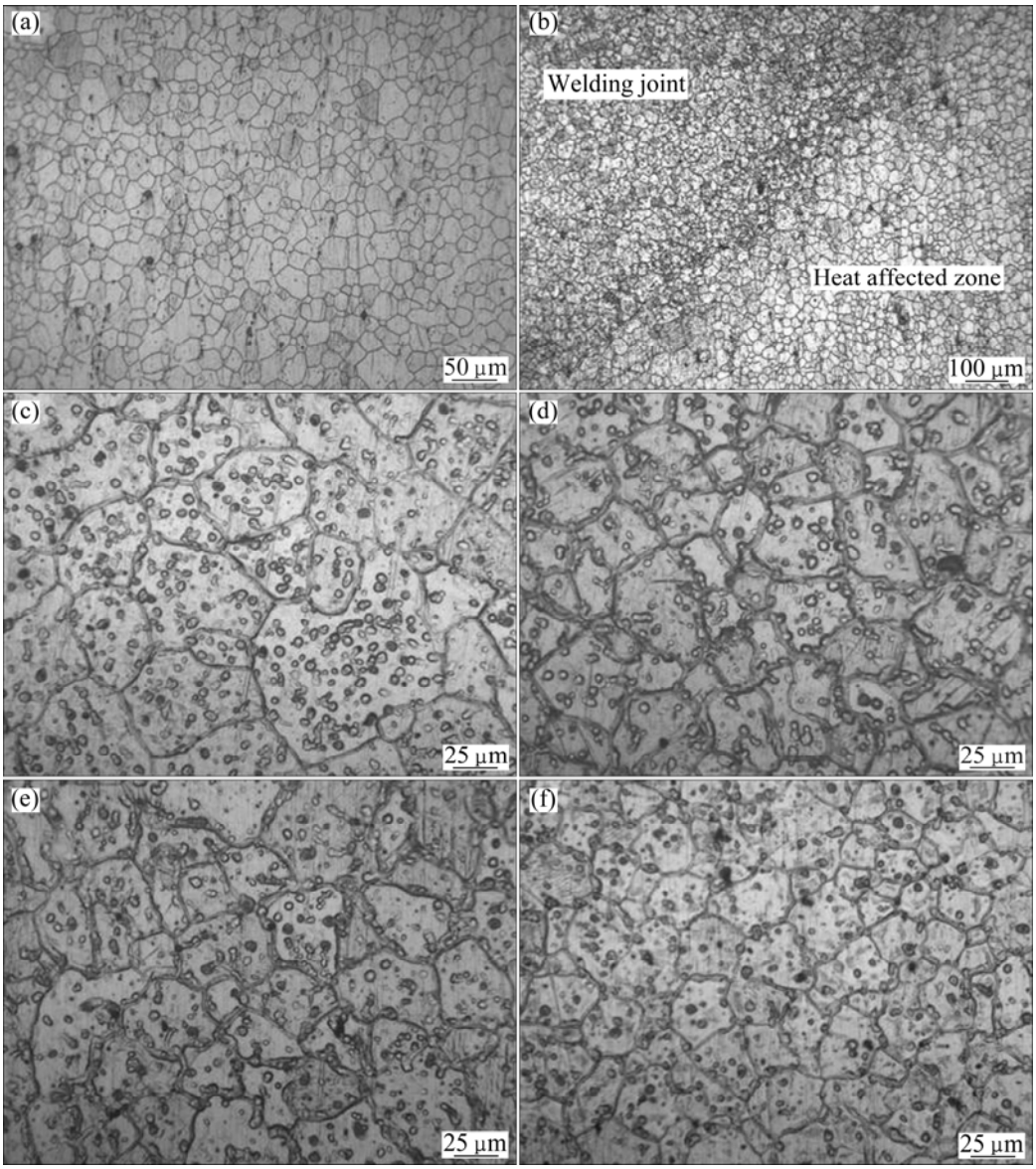

Fig. 4 Microstructures of base metal and joints welded with 25%A vibration amplitude, t=3 mm: (a) Base metal; (b) V-vib, θ=20°, welding line border; (c) No vibration, θ=0°, welding line; (d) V-vib, θ=0°, welding line; (e) H-vib, θ=0°, welding line; (f) V-vib, θ=40°, welding line

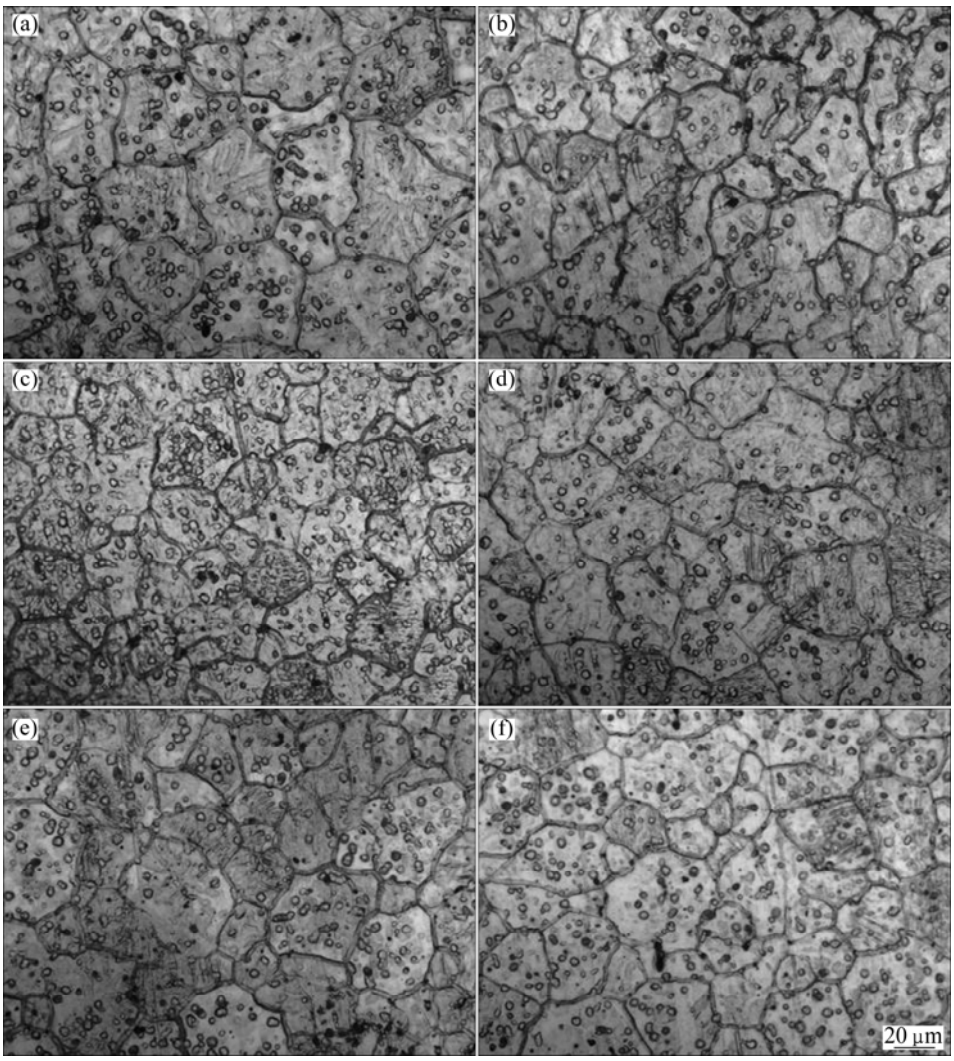

Fig. 5 Microstructures of TIG welded joints of AZ31sheet with different vibration amplitudes, t=1 mm: (a) No vibration; (b) V-vib, 12.5%A; (c) V-vib, 25%A; (d) V-vib, 37.5%A; (e) H-vib, 12.5%A; (f) H-vib, 37.5%A

It can be found that the main structure of the base metal is equiaxed grains of Mg solid solution, while in fusion zone the main structure is the quenched casting organization of small columnar crystals due to the fast cooling and crystallization. No obvious coarse structure is observed near the fusion line, indicating that the HAZ is limited. Aluminium element in AZ31 alloy is also helpful to the refinement of grains [25].

During the liquid−solid transformation of molten AZ31 alloy in the weld pool, in addition to primary α-Mg, β-phase of eutectic $Mg_{17}Al_{12}$ precipitates, as the small dispersion particles, are presented in Figs. 4 and 5. The hard and brittle β-phase can enhance the strength and lower the toughness of AZ31 alloy [25]. It can be observed that less β-phase precipitates after vibration are presented, indicating that mechanical vibration is conducive to the spread of Al element during the solidification of AZ31 alloy.

Software Image-pro® was utilized to analyze the grain size. As can be clearly seen from Fig. 6, the average diameters of grains within the joints welded with vibration are far smaller than those welded without vibration, demonstrating that vibration can greatly refine the microstructure of weldments. As shown in Fig. 6(a), minimum grain size was obtained under V-vib with groove angle of 20°. Furthermore, as shown in Fig. 6(b), level of microstructure refining increases with vibration amplitude. The phenomenon is more obvious in the welding of thick sheet, especially with the excitation of V-vib.

When external excitation is imposed on the workpiece, forced vibration of the molten metal takes place through the action of pool wall on the melt, bringing about complicated changes of thermal condition and solidification behavior of melt in the liquid pool. Theoretically, mechanism of such an action is similar to those in the vibratory casting, namely, the microstructural effects are mainly attributed to the

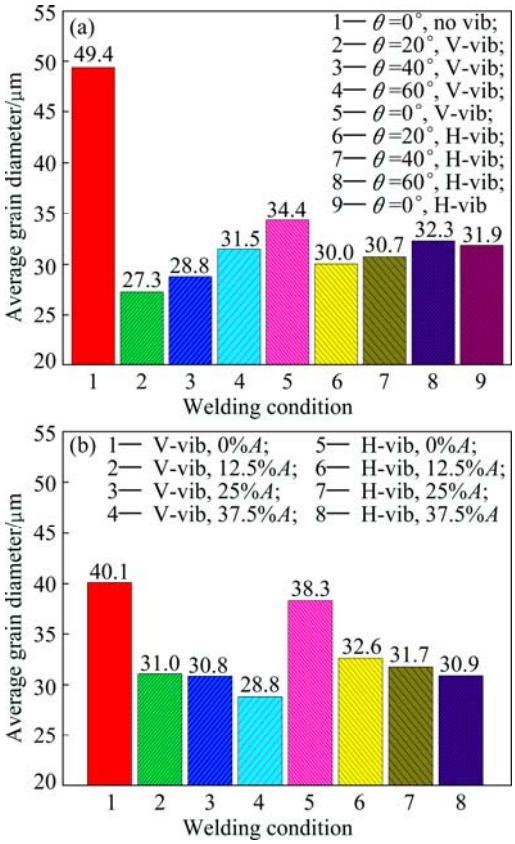

Fig. 6 Grain size of weld line under different welding conditions: (a) t=3 mm, 25%A; (b) t=1 mm, θ=0

cavitation and streaming phenomena that take place during ultrasonic treatment in the melt [17−20]. However, there are differences between vibratory welding and vibratory casting. For example, cooling time of the weld joints is very short and the HAZ is small. Meanwhile, welding arc varies periodically with the oscillation of weldment, leading to a complex thermal situation during the fusion welding. Geometry of the welding groove also affects wave transmission, e.g., different incident angles of acoustic emission lead to varying amplitudes of reflected ultrasonic L-wave (longitudinal wave) and SV-wave (vertical-shear wave) in the material, resulting in different energy transmission and attenuation contributing to the thermal condition. DAI [23] postulated that the L-wave dominates the heat transfer because of rapid energy transmission, and the SV-wave governs the heat generation due to the viscous losses associated with the energy dissipation.

The amplitude ratios of L-wave and SV-wave under different groove angles θ of the specimens can be calculated by using the equations in terms of wave propagation in elastic solids [23,26]. The characteristic curves of relative amplitude ratios A_1/A_0 and A_2/A_0 versus the incident angles for AZ31 alloy under free boundary condition and V-vib are shown in Fig. 7, where A_0 is the amplitude of the incident L-wave, A_1 is the amplitude of the reflected L-wave and A_2 is the amplitude of the reflected SV-wave.

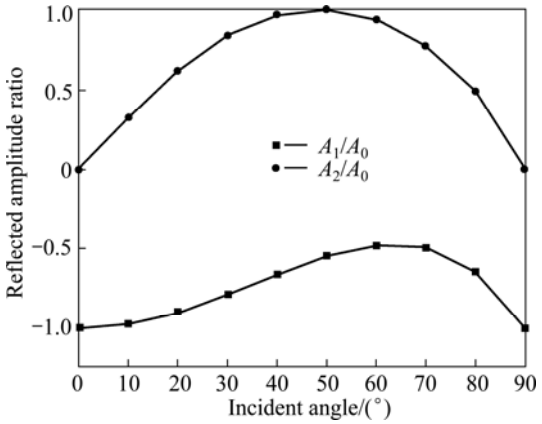

Fig. 7 Relative amplitude ratios A_1/A_0 and A_2/A_0 versus incident angles for AZ31 alloy

It can be found that the 80° incident L-wave (equal to groove angle θ of 20°) creates the largest reflected amplitude of L-wave (A_1/A_0=−0.604) and lowest reflected amplitude of SV-wave (A_2/A_0=0.489). Therefore, average grain size in the joint with θ=20° is the smallest since the highest cooling rate is generated.

3.2 Mechanical properties

According to the Hall-Petch formula, strength of metal is directly associated with its grain size. Hence, mechanical properties of the weldment would be improved since the microstructure is refined after the vibration is applied. Figure 8 illustrates the microhardness around the fusion zone of AZ31 sheet with thickness of 3 mm, from weld line center to HAZ along the transverse direction. It can be found that microhardness is improved under both horizontal and vertical vibrations, while V-vib improves the microhardness more. Therefore, though less phase β precipitates with the application of vibration in welding, it is insufficient to reduce the strength improved by grain-refinement.

Tensile test was employed to compare the mechanical properties of weld zone. The tests were conducted on a SANS CMT 5015 electronic universal testing machine with constant tensile speed of 2 mm/min. To eliminate the effect of geometry irregularity of weld seams on the testing results, positions of weld seams with full welding penetration on the plate were selected and the joints were polished smooth to obtain the same shape and size of the tensile samples, as shown in Fig. 9(a).

Figures 9(b) and (c) present the tensile curves of AZ31 weldments with thickness of 1 mm. Figure 10 shows effect of vibration (25%A) on tensile properties

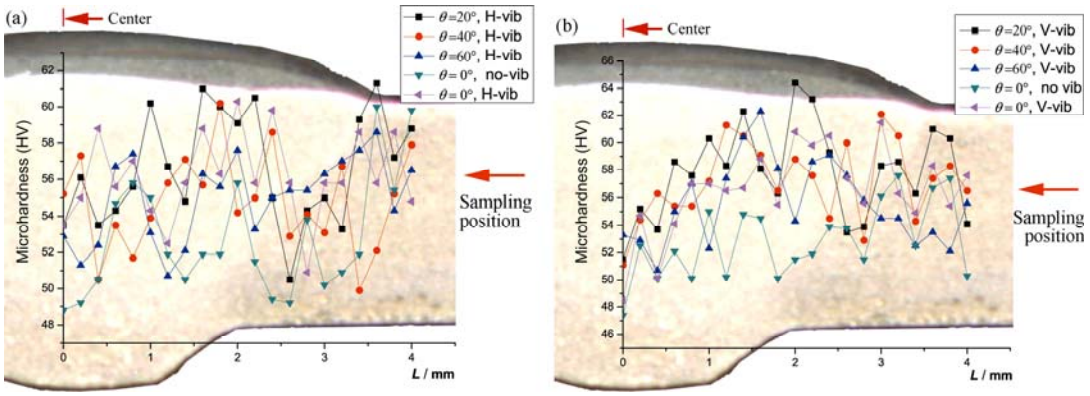

Fig. 8 Microhardness of TIG weld joints of AZ31 sheet with t=3 mm under different vibrating conditions and 25%A: (a) H-vib; (b) V-vib

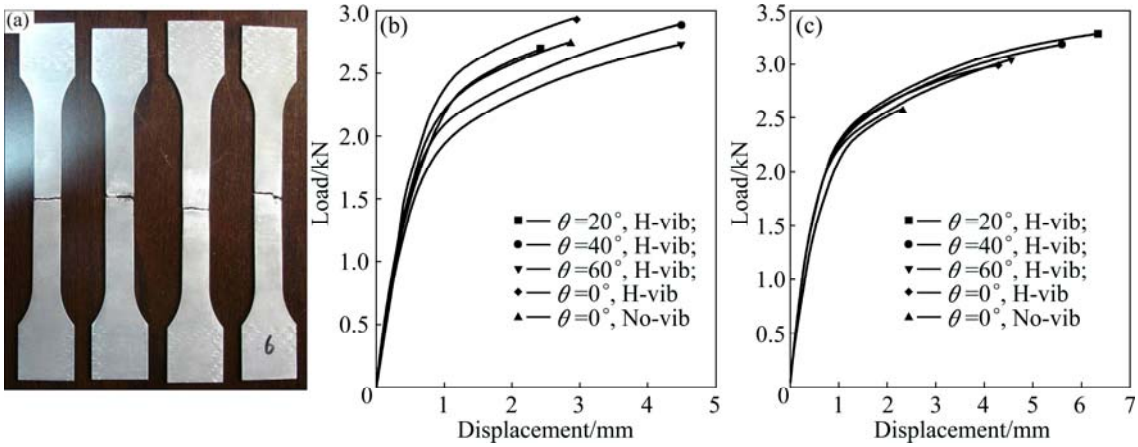

Fig. 9 Results of tensile test of TIG weldment under different conditions, t=1 mm and 25%A: (a) Tensile samples; (b) H-vib; (c) V-vib

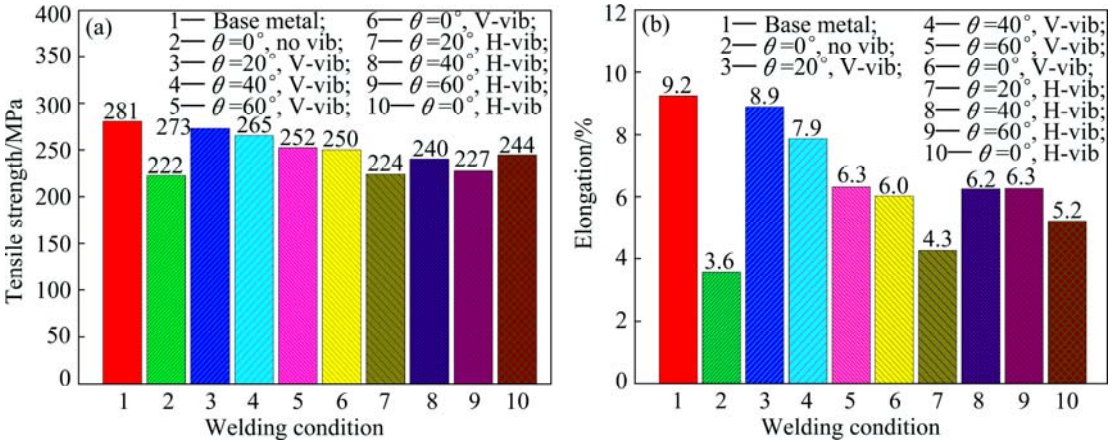

Fig. 10 Effect of vibrating parameters on tensile performance of weldments AZ31 sheet with thickness of 1 mm at 25%A: (a) Tensile strength; (b) Elongation

of AZ31 sheets with 1 mm thickness under different welding conditions. Average value from three samples are used in the statistics. Almost all the fracture positions locate in the HAZ near fusion lines and the ultimate strength and elongation of the welded samples drop in comparison with those of the parent metal. Nevertheless, the ultimate strength and elongation of welded samples are improved by the adoption of vibration. Moreover, the strength and elongation increase more with V-vib. Corresponding to the microstructure variations, mechanical properties of the welded samples reach the largest at welding groove angle of 20°.

The improvement of mechanical properties of weld joints is mainly a result of grain refinement. Besides, vibration would speed up the convection of melt in the weld pool and hence, bubbles and impurities are easy to rise and removal of hydrogen is thorough during the crystallization. Consequently, such defects as porosity and slag are reduced and macro segregation in the fusion zone decreases due to the wider turbulent layer.

4 Conclusions

1) With the application of vibration, microstructure of the AZ31 TIG welding joints is markedly refined. Average diameters of the grains within the joints decrease from 49.4 μm (welded without vibration) to 27.3−34 μm (welded with varying vibration conditions). Meanwhile, the amount of the second phase β within the fusion zone decreases slightly, and the microhardness of the joints, macroscopic tensile strength and elongation of the weldments increase.

2) The degree of microstructure refining increases with increasing the amplitude of vibration. Corresponding to the microstructure, mechanical properties of the welded samples reach the largest at welding groove angle of 20° under V-vib due to the highest cooling rate. The effect of vibration on the microstructure and mechanical performances of weld joints is more obvious for thick plate.

3) As a whole, the influence of vibration on microstructure and mechanical properties of weld joints is intrinsically related to the thermal condition and solidification behavior of the molten metal. It is affected by the wave energy transferring in the molten pool and depends on the processing and geometric parameters such as vibration amplitude, vibration direction, thickness and groove angles of the sheets.

References

[1] LIU Xu-he, GU Shi-hai, WU Rui-zhi, LENG Xue-song, YAN Jiu-chun, ZHANG Mi-lin. Microstructure and mechanical properties of Mg−Li alloy after TIG welding [J]. Transactions of Nonferrous Metals Society of China, 2011, 21(3): 477−481.

[2] TSAI T C, CHOU C C, TSAI D M, CHIANG K T. Modeling and analyzing the effects of heat treatment on the characteristics of magnesium alloy joint welded by the tungsten-arc inert gas welding [J]. Materials and Design, 2011, 32(8−9): 4187−4194.

[3] HE Zhen-bo, PENG Yong-yi, YIN Zhi-min, LEI Xue-feng. Comparison of FSW and TIG welded joints in Al−Mg−Mn−Sc−Zr alloy plates [J]. Transactions of Nonferrous Metals Society of China, 2011, 21(8): 1685−1691.

[4] ZHANG H T, SONG J Q. Microstructural evolution of aluminum/magnesium lap joints welded using MIG process with zinc foil as an interlayer [J]. Materials Letters, 2011, 65(21−22): 3292−3294.

[5] CAMPANELLI L C, SUHUDDIN U F H, ANTONIALLI A Í S, SANTOS J F, ALCÂNTARA N G, BOLFARINI C. Metallurgy and mechanical performance of AZ31 magnesium alloy friction spot welds [J]. Journal of Materials Processing Technology, 2013, 213(4): 515−521.

[6] LIU L M, REN D X. Effect of adhesive on molten pool structure and penetration in laser weld bonding of magnesium alloy [J]. Optics and Lasers in Engineering, 2010, 48(9): 882−887.

[7] CAO X, JAHAZI M, IMMARIGEON J P, WALLACE W. A review of laser welding techniques for magnesium alloys [J]. Journal of Materials Processing Technology, 2006, 171(2): 188−204.

[8] LUO Yi, YE Hong, DU Chang-hua, XU Hui-bin. Influence of focusing thermal effect upon AZ91D magnesium alloy weld during vacuum electron beam welding [J]. Vacuum, 2012, 86(9): 1262−1267.

[9] BEHRAVESH S B, JAHED H, LAMBERT S. Characterization of magnesium spot welds under tensile and cyclic loadings [J]. Materials and Design, 2011, 32(10): 4890−4900.

[10] MORDYUK B N, PROKOPENKO G I. Ultrasonic impact peening for the surface properties' management [J]. Journal of Sound and Vibration, 2007, 308(3−5): 855−866.

[11] CARBONI M, MORONI F. Tensile-shear fatigue behavior of aluminum and magnesium lap-joints obtained by ultrasonic welding and adhesive bonding [J]. Procedia Engineering, 2011, 10: 3561−3566.

[12] WATANABE T, SAKUYAMA H, YANAGISAWA A. Ultrasonic welding between mild steel sheet and Al−Mg alloy sheet [J]. Journal of Materials Processing Technology, 2009, 209(15−16): 5475−5480.

[13] SIDDIQ A, GHASSEMIEH E. Thermomechanical analyses of ultrasonic welding process using thermal and acoustic softening effects [J]. Mechanics of Materials, 2008, 40(12): 982−1000.

[14] SHAKIL M, TARIQ N H, AHMAD M, CHOUDHARY M A, AKHTER J I, BABU S S. Effect of ultrasonic welding parameters on microstructure and mechanical properties of dissimilar joints [J]. Materials and Design, 2014, 55(3): 263−273.

[15] PATEL V K, BHOLE S D, CHEN D L. Influence of ultrasonic spot welding on microstructure in a magnesium alloy [J]. Scripta Materialia, 2011, 65(10): 911−914.

[16] PATEL V K, BHOLE S D, CHEN D L. Ultrasonic spot welded AZ31 magnesium alloy: Microstructure, texture, and lap shear strength [J]. Materials Science and Engineering A, 2013, 569(1): 78−85.

[17] PUGA H, COSTA S, BARBOSA J, RIBEIRO S, PROKIC M. Influence of ultrasonic melt treatment on microstructure and mechanical properties of $AlSi_9Cu_3$ alloy [J]. Journal of Materials Processing Technology, 2011, 211(11): 1729−1735.

[18] ZHANG Zhi-qiang, LE Qi-chi, CUI Jian-zhong. Microstructures and mechanical properties of AZ80 alloy treated by pulsed ultrasonic vibration [J]. Transactions of Nonferrous Metals Society of China. 2008, 18(s1): s113−s116.

[19] AGHAYANI M K, NIROUMAND B. Effects of ultrasonic treatment on microstructure and tensile strength of AZ91 magnesium alloy [J]. Journal of Alloys and Compounds, 2011, 509(1): 114−122.

[20] LU Qing-hua, CHEN Li-gong, NI Chun-zhen. Improving welded valve quality by vibratory weld conditioning [J]. Materials Science and Engineering A, 2007, 457(1−2): 246−253.

[21] LU Qing-hua, CHEN Li-gong, NI Chun-zhen. Effect of vibratory weld conditioning on welded valve properties [J]. Mechanics of Materials, 2008, 40(7): 565−574.

[22] PUCKO B, GLIHA V. Effect of vibration on weld metal hardness and toughness [J]. Science and Technology of Welding and Joining, 2005, 10(3): 335−338.

[23] DAI Wen-long. Effects of high-intensity ultrasonic-wave emission on

the weldability of aluminum alloy 7075-T6 [J]. Materials Letters, 2003, 57(16−17): 2447−2454.

[24] WEN Tong, WEI Li, CHEN Xia, PEI Chun-lei. Effects of ultrasonic vibration on plastic deformation of AZ31 during the tensile process [J]. International Journal of Minerals, Metallurgy and Materials, 2011, 18(1): 70−76.

[25] JU Dong-ying, HU Xiao-dong. Effect of casting parameters and deformation on microstructure evolution of twin-roll casting magnesium alloy AZ31 [J]. Transactions of Nonferrous Metals Society of China, 2006, 16(s2): s874−sS77.

[26] ACHENBACH J D. Wave propagation in elastic solids [M]. Amsterdam: North-Holland, 1999: 185−200.

高频振动对 AZ31 镁合金 TIG 焊接接头微观组织与力学性能的影响

温 彤, 刘诗尧, 陈 世, 刘澜涛, 杨 臣

重庆大学 材料科学与工程学院，重庆 400044

摘 要：设计一套能对焊件在水平和垂直方向进行频率 15 kHz、最大输出功率 2 kW 激振的 TIG 焊装置。在此基础上，对厚度 3 mm 和 1 mm 的 AZ31 镁板在不同激振方向、激振振幅以及剖口形式下进行焊接，对比分析不同条件下焊接接头的组织与性能。发现激振使得 AZ31 TIG 焊缝熔合区的组织显著细化，第二相 β-$Mg_{17}Al_{12}$ 的析出减少；另外，焊缝区域显微硬度及试样的整体抗拉强度和伸长率提高；振动对厚板焊缝的影响更大，且垂直方向激振的影响更明显。振动对 AZ31 TIG 焊接接头组织与性能的影响，取决于焊接熔池金属凝固行为以及超声波激振能量的传递状态等因素，与激振振幅、方向以及焊接剖口角度和板厚等密切相关。

关键词：镁合金；TIG 焊接；振动；微观组织；力学性能

(Edited by Yun-bin HE)